Biochemical perturbations of the mitotic spindle in *Xenopus* extracts using a diffusion-based microfluidic assay

Byung-Kuk Yoo,[1,2,3,a)] Axel Buguin,[2,b)] and Zoher Gueroui[1,c)]
[1]*Ecole Normale Supérieure - PSL Research University, Département de Chimie, UMR CNRS-ENS-UPMC 8640, 24, Rue Lhomond, 75005 Paris, France*
[2]*Physico-Chimie Curie, Institut Curie, UMR CNRS-UPMC 168, 26, rue d'Ulm, F-75248 Paris Cedex 05, France*
[3]*Physical Biology Center for Ultrafast Science and Technology, Arthur Amos Noyes Laboratory of Chemical Physics, California Institute of Technology, Pasadena, California 91125, USA*

(Received 9 February 2015; accepted 24 June 2015; published online 7 July 2015)

A microfluidic device is a powerful tool to manipulate in a controlled manner at spatiotemporal scales for biological systems. Here, we describe a simple diffusion-based assay to generate and measure the effect of biochemical perturbations within the cytoplasm of cell-free extracts from *Xenopus* eggs. Our approach comprises a microliter reservoir and a model cytoplasm that are separated by a synthetic membrane containing sub-micrometric pores through which small molecules and recombinant proteins can diffuse. We have used this system to examine the perturbation of elements of the mitotic spindle, which is a microtubule-based bipolar structure involved in the segregation of the replicated genome to daughter cells during cell division. First, we used the small molecule inhibitor monastrol to target kinesin-5, a molecular motor that maintains the microtubule spindle bipolarity. Next, we explored the dynamics of the mitotic spindle by monitoring the exchange between unpolymerized and polymerized tubulin within microtubule fibers. These results show that a simple diffusion-based system can generate biochemical perturbations directly within a cell-free cytoplasm based on *Xenopus* egg extracts at the time scale of minutes. Our assay is therefore suitable for monitoring the dynamics of supramolecular assemblies within cell-free extracts in response to perturbations. This strategy opens up broad perspectives including phenotype screening or mechanistic studies of biological assembly processes and could be applied to other cell-free extracts such as those derived from mammalian or bacterial cells.
[http://dx.doi.org/10.1063/1.4926324]

INTRODUCTION

Manipulating the environment of biological assemblies at various spatiotemporal scales is a key for understanding their functional properties. In this regard, a microfluidic device offers powerful tools to modify the extracellular environment in a controlled manner through the use of concentration gradient generators.[1–4] These methods allow the manipulation of liquid solutions of varying compositions to rapidly and locally change the conditions in a small-scale system and monitor the resulting kinetic evolution. To control the extracellular environment of cells (bacteria or migrating cells), such strategies generally rely on the application of a hydrodynamic flow and require immobilized or adhering cells. Alternative strategies involve the

[a)]bkyoo@caltech.edu
[b)]Axel.Buguin@curie.fr
[c)]Author to whom correspondence should be addressed. Electronic mail: zoher.gueroui@ens.fr. Tel.: +33144322409. Fax: +33144323858.

generation of a concentration gradient based on the diffusion of stimuli within the microenvironment of cells, for which hydrodynamic flows are not suitable.[5–8] Controlling the concentration directly within the cell cytoplasm requires the use of cell permeant molecules[9] or other approaches such as optogenetics[10] or nanomanipulation tools such as magnetic nanoparticles.[11–13] Here, we have devised a diffusion-based method to generate spatiotemporal perturbations of exogenous proteins or specific chemical drugs directly within the cell cytoplasm. Our approach comprises a microliter reservoir and a model cytoplasm that are separated by a synthetic membrane containing sub-micrometric pores through which small molecules and recombinant proteins can diffuse. This *in vitro* microfluidic device allows temporal perturbations to be generated through the diffusion of small chemicals or recombinant regulatory proteins within minutes. In contrast to conventional microfluidic systems that use hydrodynamic flows, this system provides simplicity and avoids the mechanical disruption of biological assemblies within the cytoplasm (Figure 1(a)).

To validate our approach, we used the device to investigate the temporal perturbation of key elements of the mitotic spindle, which is a microtubule-based bipolar structure involved in the segregation of the replicated genome to daughter cells during cell division.[14] For our model cytoplasm, we selected *Xenopus* egg extracts as they are a powerful system for dissecting cytoskeleton morphogenesis during meiosis and mitosis.[15] They permit biochemical manipulations (e.g., the depletion or addition of drugs) and cell-cycle control while offering very good optical properties compared with the difficulties inherent in the imaging of large embryonic cells.[16,17] The techniques to examine spindle dynamics are mainly based on fluorescent-based measurements such as speckle measurements and quantitative polarized light microscopy.[18,19] Tracking

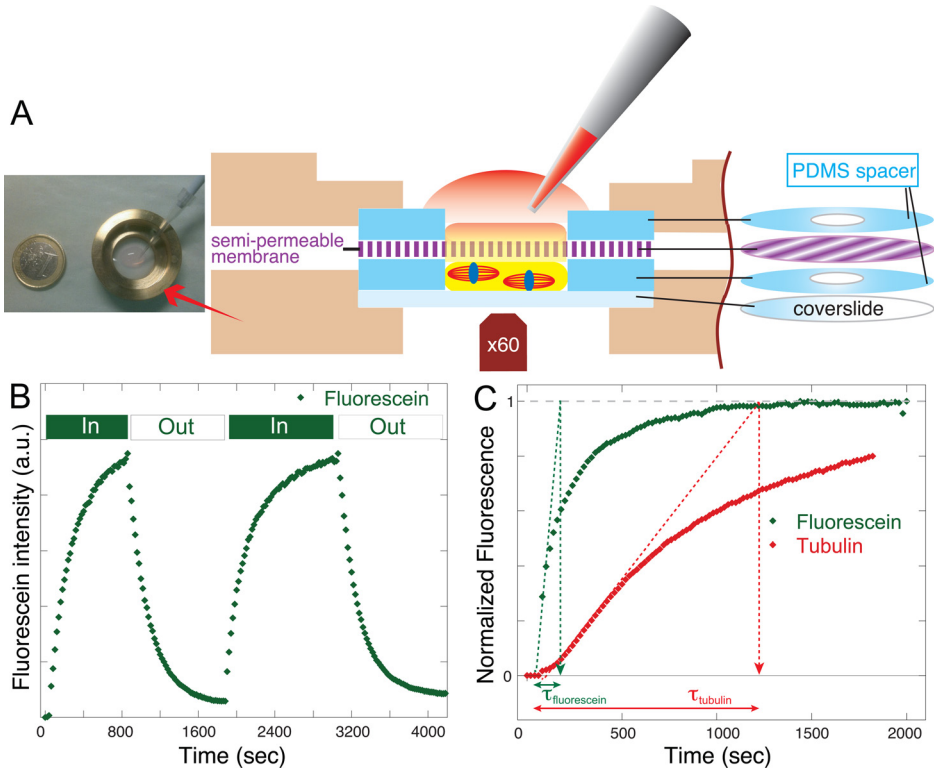

FIG. 1. Principle of the diffusion-based assay and the time-dependent change in fluorescein concentration monitored using fluorescent microscopy. (a) Schematic illustration of the diffusion-based microfluidic device. *Xenopus* egg extract containing mitotic spindles is shown in yellow. (b) Intensity profile of fluorescein molecules diffusing throughout the membrane results in a monotonic change in fluorescence in the observation chamber. The addition of fluorescein solution results in an increase in fluorescence, whereas the subsequent addition of a non-fluorescent solution leads to a reduction in fluorescence in the observation chamber. (c) Intensity profile of fluorescently labeled tubulin (tetramethylrhodamine (TRITC)-tubulin) and fluorescein.

the behavior of individual protein molecules in spindles reveals also the complex dynamics of the microtubule structures.[20] Additionally, conventional approaches for perturbing spindle assembly in egg extracts rely on adding the reagents (small molecules, proteins) to a tube of extract, mixing, and then monitoring the dynamic after deposition on a coverslide.[21] With our diffusion-based assay, we first tested the effect of the small molecule monastrol that targets kinesin-5, a molecular motor involved in maintaining the microtubule spindle bipolarity. Second, we examined the dynamics of the mitotic spindle by monitoring the exchange between the tubulin cytoplasmic pool and polymerized tubulin within microtubule fibers.

RESULTS AND DISCUSSION

Design and characterization of the diffusion-based assay in *Xenopus* egg extracts

Biochemical perturbation of the egg extract through the addition of chemicals or proteins needs to be performed in a non-invasive way to avoid the mechanical disruption of cytoplasmic structures. Biological assemblies such as the microtubule spindle are highly fragile and would be damaged by the shear stress induced by a flow. To maintain these structures, we have therefore designed a microfluidic chamber consisting of a microliter reservoir that is connected to the *Xenopus* cell extract through a synthetic membrane containing sub-micrometric pores. Molecules of interest can be introduced into the system using a porous medium that allows the diffusion of small molecules while filtering out any hydrodynamic shearing; all flows being screened over a typical distance corresponding to the pore size.[22]

Figure 1(a) shows a schematic diagram of the diffusion-based assay. The device allows parallel observations to be made using only a small amount of material (i.e., *Xenopus* cytoplasm and the proteins of interest). It contains a closed chamber (typical height $h_c \approx 40\,\mu$m and volume $\approx 3\,\mu$l) that is in contact with a second chamber through a porous membrane. Molecules of interest were loaded into the top open area of the system by dropping 10–100 μl of sample using a pipette. The device comprises three parts: a PEGylated coverslide, a semi-permeable membrane, and a polydimethylsiloxane (PDMS)-based spacer (see Methods for details). First, we loaded the egg extracts into what will be the lower chamber (PDMS spacer was stuck onto the coverslide). Second, we continued the assembly of the chamber by sticking the membrane onto the PDMS spacer. The overall assembly was sandwiched into Ludin-like chamber. Third, we added the reagents (10–100 μl) onto the upper chamber. The volume was fixed to have 3 μl to fill the lower chamber and no leakage was observed during the course of the experiment.

To validate the assay, we studied the diffusion of small molecules within egg extracts using fluorescent dyes. After assembling the device containing cell extract in the lower chamber, the excess of cell extract in the upper chamber was gently removed by pipetting and replaced by the same cell extract supplemented with fluorescein molecules (concentration of fluorescein $c_f = 5\,\mu$M). In the porous membrane and in lower chamber (Figure 1(a), shown in yellow), the flows are screened, the fluid is at rest, and equilibrium can only be reached through the diffusion of the fluorescent molecules. Our system allows fluorescence intensity in the lower chamber to be monitored as a function of time using time-lapse microscopy (one image every 20 s; see Methods).

Figure 1(b) shows a typical variation in fluorescence intensity after a concentration jump of fluorescein within the egg extract in the lower chamber. In this experiment, non-fluorescent buffer was added to the upper chamber to remove fluorescein molecules after 800 s to illustrate how a temporal cycle of perturbations can be performed. Upon the addition of fluorescein to the upper chamber, the fluorescent molecules equilibrate only by diffusion between the two compartments. The amount of liquid outside imposes the final equilibrium concentration but not the kinetic of the process.

Ignoring details, we will show in this section that the process is indeed governed by diffusion and gives the typical time necessary for the two compartments to equilibrate. This typical time can become a limiting factor to study biological systems having a fast kinetic.

This diffusion process is governed by the first Fick's equation

$$\vec{J} = -D\vec{\nabla}c, \tag{1}$$

in which J is the flux of molecules per unit area and D is their diffusion coefficient.

At the start of the experiment ($t = 0$), the jump in fluorescein concentration between the two sides of the porous membrane is c_f and thus leads to $\| \vec{\nabla} c\|_{t=0} \sim \frac{c_f}{h_m}$. On the other side of the membrane, the flux of fluorescein molecules at $t = 0$ can be easily estimated from the evolution of the normalized fluorescence (NF, we have checked that the fluorescence intensity is directly proportional to the number n_f of fluorescein molecules) as a function of time (Figure 1(c)): this gives $J_{t=0} \sim \frac{1}{S_{eff}}\left(\frac{dn_f}{dt}\right)_{t=0} \sim \frac{1}{S_{eff}}\left(\frac{dNF}{dt}\right)_{t=0} c_f V$, in which S_{eff} is the effective surface area of the porous membrane (for membranes with cylindrical pores $S_{eff} = porosity \times S$), $V = h_c \times S$ is the volume of the lower chamber in the observation field of the microscope), and $n_f = NF(t)c_f V$. Finally, we obtain

$$D \sim \frac{1}{porosity}\left(\frac{dNF}{dt}\right)_{t=0} h_c h_m. \tag{2}$$

With a porosity of 20% and $\left(\frac{dNF}{dt}\right)_{t=0} = \frac{1}{\tau_{fluorescein}} \sim 10^{-2}\text{s}^{-1}$, this gives $D_{\text{fluorescein/cell extract}} = 50\,\mu\text{m}^2/\text{s}$, which can be compared with $D_{\text{fluorescein/water}} = 500\,\mu\text{m}^2/\text{s}$.[23] According to the Stokes-Einstein equation, our extract is ten times more viscous than water, which is in good agreement with what has been reported in the literature.[24]

In addition, we tested whether proteins could be successfully used in our assay. We deposited a solution of fluorescently labeled tubulins (110 kDa) in the upper chamber and monitored protein diffusion into the observation chamber. Figure 1(c) (the red curve) shows the temporal behavior of fluorescently labeled tubulin (initial concentration of 300 nM), which diffused within the lower chamber containing the cell extract. The temporal evolution of the intensity of fluorescence was slower for tubulin than fluorescein, which can be explained by the difference in the hydrodynamic radius of the two molecules. Using Eq. (2), $D_{\text{tubulin/cell extract}} = 5\,\mu\text{m}^2/\text{s}$ and $\left(\frac{dNF}{dt}\right)_{t=0} = \frac{1}{\tau_{tubulin}} \sim 10^{-3}\text{s}^{-1}$, which are in good agreement with *in vivo* measurements of $D_{\text{tubulin}} \sim 6\,\mu\text{m}^2/\text{s}$.[25]

Perturbation of spindle morphogenesis

We next examined whether the biofunctionality of *Xenopus* egg extracts is conserved during the assay by monitoring the assembly and maintenance of the microtubule spindle. To assemble bipolar microtubule spindles, we incubated purified chromosomes in metaphase egg extracts of *Xenopus* oocytes for 45 min.[16] This cell-free system has been used extensively to examine the mechanisms of bipolar spindle assembly[21] and is compatible with microfluidic and biophysical manipulations.[11,26,27] The formation of the bipolar spindles after 45 min (steady state) is depicted in Figure 2(a). They have similar morphometric properties to bulk spindles (Figure 2(b)).

Next, we used the diffusion-based assay to monitor the effect of the inhibition of the kinesin-5 Eg5, which is a tetrameric motor involved in the maintenance of bipolarity.[16,28] In particular, the inhibition of Eg5 by the small molecule monastrol is known to induce morphological defects in the spindle by forming collapsing mono-asters instead of bipolar structures (Figure 2(d), inset). Within a few minutes of adding monastrol to our assay, time-lapse acquisitions using confocal microscopy revealed a transition from a bipolar spindle to a mono-polar structure (Figure 2(c)). Temporal evolution of the spindle length (pole-to-pole distance) for six representative spindles shows a 50% reduction in length within 6–13 min, which corresponds to a shortening rate of approximately 1–2 μm/min (Figure 2(d) and Figure S1 (see supplementary material in Ref. 29)). Control experiments show that the spindle remains unchanged in the absence of perturbations in the chamber (Figure 2(e)). Altogether, these results suggest that our assay is suitable for monitoring the dynamics of supramolecular assemblies within cell-free extracts and could be used, for example, to assess the response to drugs.

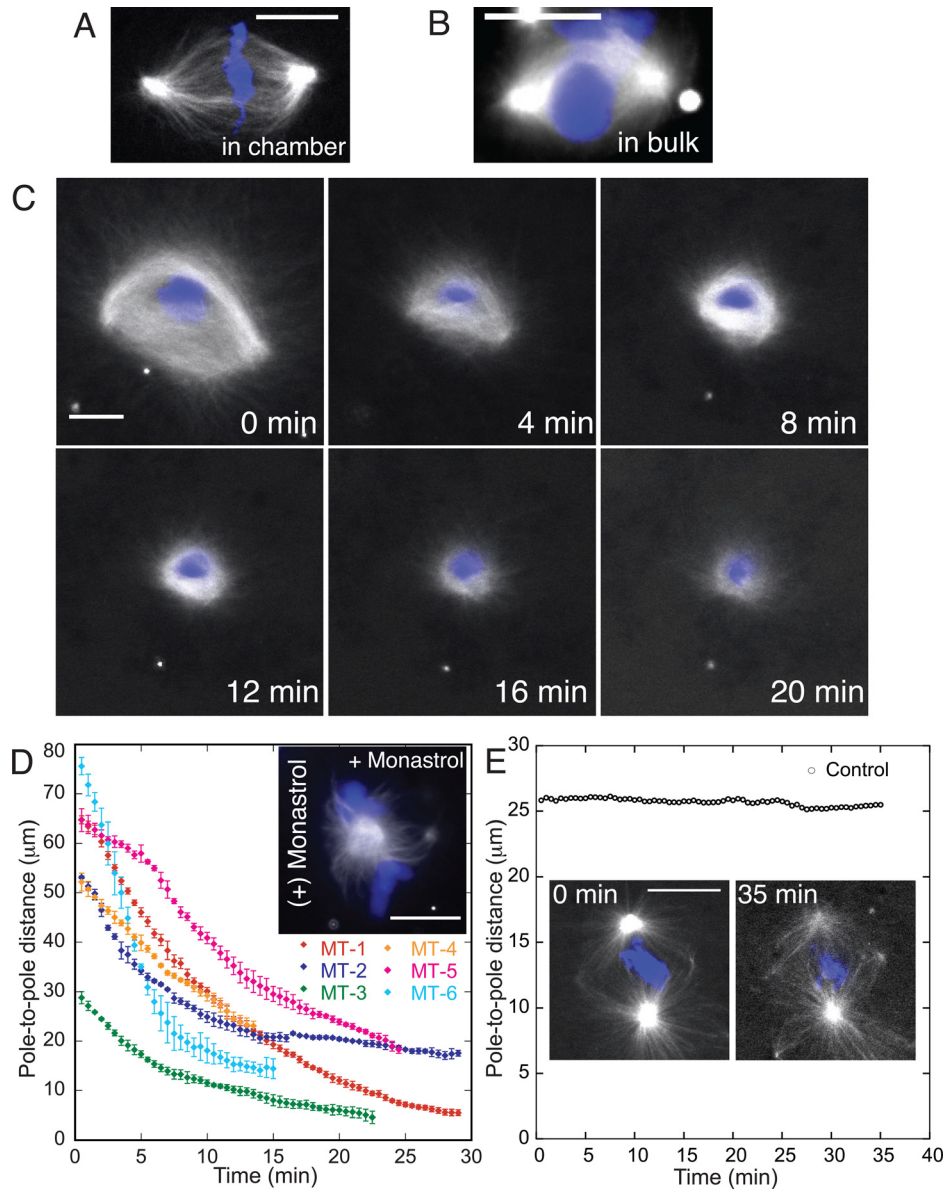

FIG. 2. Temporal perturbations of spindle morphogenesis. (a) Bipolar spindle structure formed in the diffusion-based assay and (b) in bulk (control). Spindles were visualized with fluorescently labeled tubulin (X-rhodamine) and chromosomes with DAPI (blue). (c) Monastrol perturbations induce changes in spindle morphometry: time-lapse observation of the meiotic spindle upon addition of monastrol (final concentration of ∼200 μM). (d) Evolution of the spindle pole-to-pole as a function of time upon monastrol perturbation (six independent experiments) reveals the shrinking of the spindle structure. Scale bars: 20 μm. (e) Control experiments show that the spindle remains stable in the absence of perturbations in the chamber.

Dynamics of tubulin within microtubule spindles

We also used our assay to examine tubulin dynamics within microtubule spindles. It is well known that microtubule fibers are highly dynamic polymers and exhibit both dynamic instability and constant polymerization/depolymerization that renews the tubulin dimers within the fibers.[30] Monitoring the incorporation of tubulin dimers would provide insights into the dynamics of tubulin exchange within microtubule spindles. We therefore investigated how a concentration jump of labeled tubulins is incorporated into microtubule spindles maintained at steady state (Figure 3). We designed an experiment in which red-labeled tubulins are incorporated into pre-assembled spindles labeled with green tubulin (Figure 3(b)). Figure 3(a) reports a

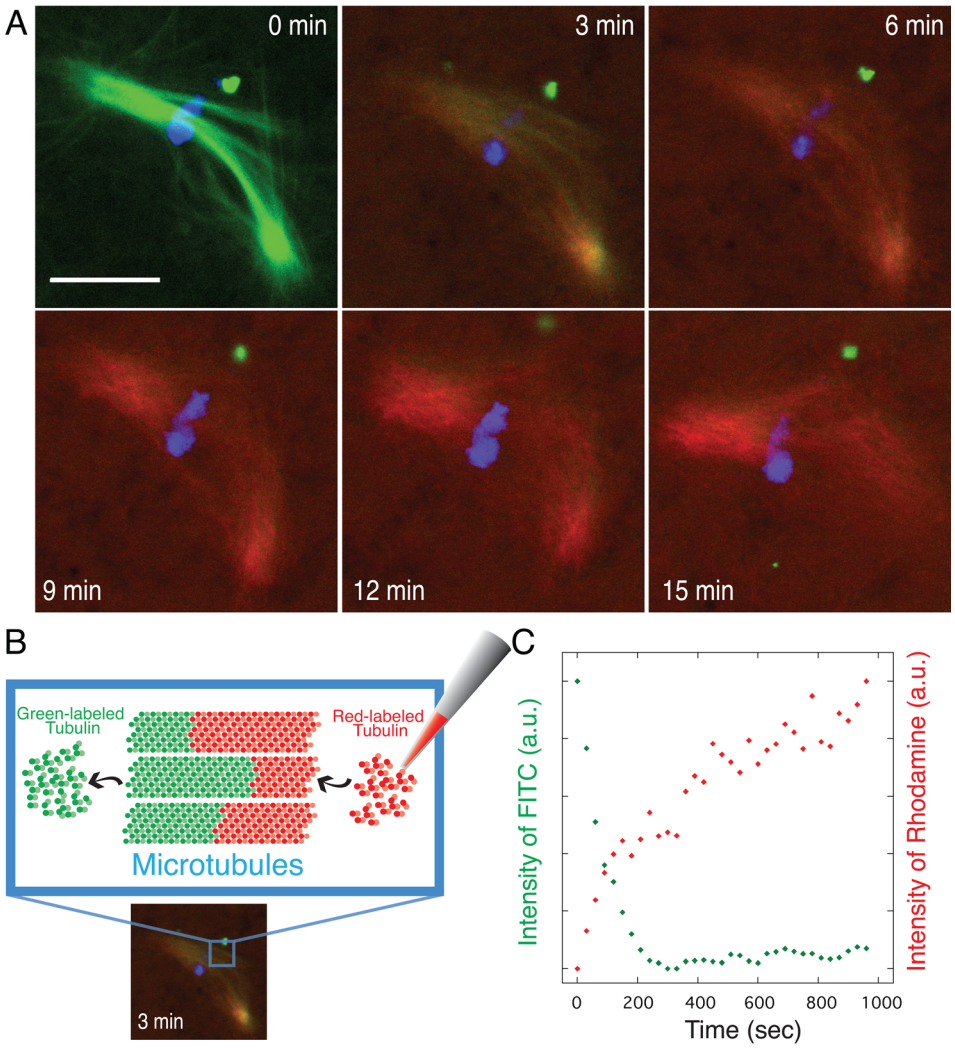

FIG. 3. Diffusion of small proteins: dynamics of tubulin within microtubule spindles. (a) Time-lapse acquisition of the dynamics of tubulin exchange within the spindle in three channels (green, red, and merge). Green: FITC-labeled tubulin, red: X-rhodamine-labeled tubulin, and blue: chromosomes stained with DAPI. Scale bar: 20 μm. (b) Principle of the treadmilling experiment: tubulin exchange within microtubule fibers. (c) Temporal evolution of the intensity of FITC-labeled tubulin (green) and X-rhodamine-labeled tubulin (red) performed on the entire spindle. Both curves are normalized at steady-state.

time-lapse sequence of the dynamics of tubulin exchange within the spindle. The separate time courses from each channel (green, red, and merge) show the change in intensity induced by the red-labeled tubulin. In this example, red-labeled tubulins were detected within the microtubule spindle 1–3 min after their injection into the upper chamber, suggesting a rapid polymerization of cytoplasmic tubulin within the microtubule–based spindle. In parallel to the incorporation of red-labeled tubulins (as shown by the increase in intensity of the red signal), we observed a dissociation of green-labeled tubulins from the microtubule fibers (revealed by a decrease in the intensity of the green signal). After 10 min, the spindle was completely renewed and fully composed of red-tubulin.

The quantification of fluorescence intensity for five different spindle assemblies shows a large variability in the tubulin dynamics (Figures 4(a) and 4(b)). For instance, tubulin dynamics increased by 50% in the spindle within a timescale of 200–1000 s. In Figure S2, the regions of interest (ROIs) 1 and 2 report the measurement of the change in intensity in tubulin signal in an area containing a half-spindle, e.g., microtubules bridging the chromosomes to the pole (see

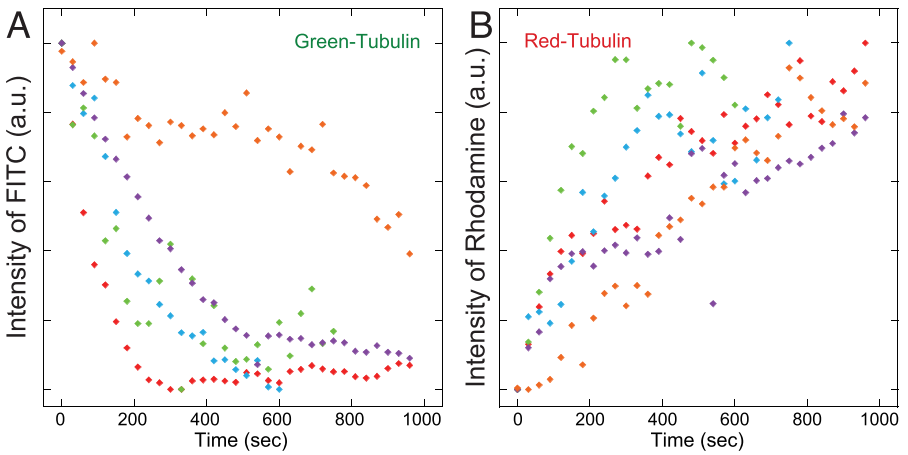

FIG. 4. Dynamics of tubulin within microtubule spindles. Five independent measurements of tubulin dynamics: temporal evolution of the intensity of FITC-labeled tubulin (left) and X-rhodamine-labeled tubulin (right) performed on the entire spindle.

supplementary material, Ref. 29). The associate ROI focuses on the polymerization dynamic of an array of polarized microtubules having their plus end pointed towards the chromosomes and their minus-end towards one of the spindle poles. Therefore, our data suggest that both half-spindle behave the same in term of polymerization, suggesting no strong asymmetry in the internal flow dynamic of the spindle regarding to the chromosome metaphase plan. Heterogeneity in spindle formation (time required to complete assembly, variability spindle morphology), attributed to intrinsic fluctuations (arising during microtubule and molecular motor self-organization) and also to extrinsic fluctuations (such as heterogeneity due to cell extract preparations), could explain the variability observed in the tubulin dynamics.

The rates of intensity changes depend on two main coupled mechanisms: the polymerization/depolymerization rates of the microtubule fibers and the diffusion of red-labeled tubulin through the membrane to the cytoplasmic chamber. This suggests that tubulin dimers have a life-time of 3–10 min within the spindle structures, which maintain a constant morphology at steady state over a much longer period (60 min). The rapid turnover rate of tubulin within spindle structures may partly explains how the cell-division apparatus has the remarkable ability to maintain a steady-state morphology over time while still being able to disassemble or re-assemble rapidly depending on the progression of the cell cycle.[30–32]

CONCLUSIONS

We have demonstrated how a simple diffusion-based assay based on *Xenopus* egg extracts allows biochemical perturbations to be generated directly in a cell-free cytoplasm within minutes. These results suggest that our assay is suitable for monitoring the dynamics of the perturbation response of supramolecular assemblies within cell-free extracts.

From a cell biophysic's perspective, our approach could provide useful tools to examine how the mitotic spindle apparatus is able to accommodate environmental fluctuations (for example, variations in regulatory protein concentration) to confer the adaptation or the robustness necessary for cell proliferation. This is highly relevant since defects or disruption of the mitotic spindle formation can lead to morphogenetic defects of the cell division apparatus that can be related to the development of cellular anomalies and eventually various cancers. In particular, targeting the numerous proteins, including motor proteins, required for proper cell division that were recently discovered, will allow us to quantify the dynamics of spindle assembly to examine the robustness of the mitotic spindle with both mechanistic and system level perspectives. This strategy opens up broad perspectives including phenotype screening or

mechanistic studies of biological assembly processes and could be applied to other cell-free extracts such as those derived from mammalian or bacterial cells.

METHODS

Assembly of the diffusion-based microfluidic assay

The chamber assay comprises three parts: a PEGylated coverslide, a semi-permeable membrane, and a PDMS-based spacer (Figure 1(a)). The coverslide was coated with a polyethylene glycol-grafted poly-L-lysine polymer (PLL-g-PEG) to prevent non-specific interactions. First, a few microliters of PLL-g-PEG [1 mg/ml, SuSos AG, Switzerland, PLL (20 kDa) grafted with PEG (2 kDa), g = 3.0–4.0] was gently spread on the surface of a clean coverslip (VWR, 24 mm) for 1 h and washed with distilled water and dried in the air with blocking outer airflow. We chose commercially available PDMS-like film, as spacer, called "Gel-Film" (38 μm thick, Gel-Pak, Hayward, CA 94544). The volume of the chamber was adjusted by punching the film to the desired chamber geometry (2 mm diameter). The protected layer of Gel-Film was removed and placed on the coverslip. We used polycarbonate membranes (Millipore, Inc., pore size: 0.22 μm; thickness: 25 μm; diameter: 25 mm; and porosity: 20% (manufacturer's data)) as semi-permeable membranes that were initially incubated with phosphate buffered saline (PBS) for 1 night and subsequently dried. The membrane was placed gently on the PDMS spacer, and we used a stainless steel chamber (Ludin-like chamber) to tighten together the different layers. The volume of the sample to be injected into the chamber was adjusted to be slightly more than the chamber volume and the sample spread within the chamber to fill it. Small molecules and proteins of interest were loaded into the top chamber by dropping 10–100 μl of sample using a pipette. Before adding the medium containing the small molecules, or the proteins, we gently aspirate the solution present in the upper chamber. The amount of liquid outside imposes the final equilibrium concentration but not the kinetic of the process (in Eq. (2), NF is a normalized fluorescence, e.g., a fluorescence intensity divided by the fluorescence at equilibrium.). All the experiments were performed in a close chamber keeping constant the humidity to avoid evaporation problems. To determine the diffusion coefficient of dye molecules and fluorescent proteins, we added *Xenopus* egg extracts in the observation chamber and complemented extracts with and without the molecules of interest in the top chamber. We monitored the temporal evolution of intensity using fluorescence microscopy by acquiring signals just above the coverslip–-solution interface. During the transient regime, a spatial variation in concentration over the chamber height is established. In our experiments, we have restrained our study to a specific position in the z-axis (just above the coverslide), allowing us to focus on the spindle based-structures and to perform our measurements in a reproducible manner. Since we are using epi-fluorescence observations, the fluorescence is integer all over the lower chamber thickness.

Xenopus egg extract preparation and microtubule-based structure self-organization in cell extracts and reagents

Cytostatic-factor-arrested (CSF) *Xenopus laevis* egg extracts, which correspond to "active" cytoplasm of oocytes arrested in metaphase II of meiosis, were prepared as previously described.[15] Briefly, egg extracts are prepared from the African claw-toed frog (*Xenopus laevis*), which produces unfertilized eggs. Once laid, *Xenopus laevis* eggs are collected in an arrested metaphase of meiosis II by an activity called CSF. After collecting, dejellyied eggs are first packed and then crushed by centrifugation. Fractionated extracts containing separated layers of lipid droplets, cytoplasm, and finally yolk granules as well as nuclei were obtained by separating them out via centrifugation. We carefully removed the cytoplasm that has an optimal activity for 6–8 h when kept on ice. Monastrol, adenosine triphosphate (ATP), dithiothreitol (DTT), creatine phosphate, and creatine phosphokinase were purchased from Sigma-Aldrich (St. Louis, MO). Tubulins, labeled with X-rhodamine or with fluorescein isothiocyanate (FITC), were prepared as previously described[12] and used at ~200 nM for imaging microtubule distribution. Microtubule structures were assembled using metaphase extracts in the presence of tubulin

dyes. *Xenopus* cell extracts were incubated with labeled tubulin (200 nM final), DTT (2 mM final), and an ATP-regenerating system (1 mM ATP, 10 mM creatine phosphate, 100 μg/μl creatine phosphokinase, and final concentrations). All reagents were freshly made for each measurement and all experiments were performed in metaphase extracts in a temperature-controlled room at 20 °C.

Perturbations of spindle assembly mediated by monastrol and tubulin-exchange experiments

The spindle-assembly processes were performed in tubes and in the chamber. The extracts (3 μl s) were transferred to the chamber assay 45–50 min after spindle formation. Once spindle assemblies were localized, a mixture of cell extract containing monastrol (50 μM) was added to the upper chamber. For the tubulin-exchange experiment, we used two mixtures of cell extract: FITC-labeled tubulin used for the initial spindle morphogenesis completion was added to the lower observation chamber and rhodamine-labeled tubulin was placed in the upper chamber compartment.

Fluorescent imaging and data analysis

Fluorescence imaging of microtubule asters was performed using an inverted microscope (IX81, Olympus), with either a 60× (PlanApochromatic, NA 1.42, oil-immersion) or 40 × (UPlanFLN, NA 1.30, oil-immersion) objective, and an electron multiplying CCD (EM-CCD) camera (C9100–02, Hamamatsu). Microscope settings and functions were controlled using Simple PCI software (Hamamatsu). Image analysis was performed using ImageJ (NIH) and Simple PCI software. Confocal microscopy was used to examine time-lapse dynamics of the mitotic spindle response and was performed with a Zeiss LSM 710 laser scanning confocal microscope using a 63× (PlanApochromatic, NA 1.4) objective. Image analysis was performed using LSM software Zen 2009 together with ImageJ. The intensity values were measured by computing the mean intensity over the region of interest (total spindle area, ROI, etc.). This value was then corrected from the fluorescent background of the cytoplasm and normalized.

ACKNOWLEDGMENTS

We thank Mathieu Morel for careful reading of the manuscript. This work was supported by the Foundation Pierre-Gilles de Gennes (FPGG), CNRS, Ville de Paris "Emergence(s)," FRM (ING20150532742), and Ecole Normale Supérieure. B.-K.Y. is a Ligue contre le cancer (LCC) postdoctoral fellow.

The authors declare that they have no competing interests.

NOMENCLATURE

DAPI	4′,6-diamidino-2-phenylindole
Nf	normalized fluorescence
PLL-g-PEG	polyethylene glycol-grafted poly-L-lysine polymer

[1]N. L. Jeon, S. K. W. Dertinger, D. T. Chiu, I. S. Choi, A. D. Stroock, and G. M. Whitesides, Langmuir **16**, 8311 (2000).
[2]V. V. Abhyankar, M. A. Lokuta, A. Huttenlocher, and D. J. Beebe, Lab Chip **6**, 389 (2006).
[3]E. Berthier and D. J. Beebe, Lab Chip **14**, 3241 (2014).
[4]D. M. Cate, C. G. Sip, and A. Folch, Biomicrofluidics **4**, 44105 (2010).
[5]S.-Y. Cheng, S. Heilman, M. Wasserman, S. Archer, M. L. Shuler, and M. Wu, Lab Chip **7**, 763 (2007).
[6]M. Morel, D. Bartolo, J.-C. Galas, M. Dahan, and V. Studer, Lab Chip **9**, 1011 (2009).
[7]G. Charvin, F. R. Cross, and E. D. Siggia, PLoS One **3**, e1468 (2008).
[8]F. Evenou, J.-M. Di Meglio, B. Ladoux, and P. Hersen, Lab Chip **12**, 1717 (2012).
[9]B. Lin, W. R. Holmes, C. J. Wang, T. Ueno, A. Harwell, L. Edelstein-Keshet, T. Inoue, and A. Levchenko, Proc. Natl. Acad. Sci. U. S. A. **109**, E3668 (2012).
[10]J. E. Toettcher, C. A. Voigt, O. D. Weiner, and W. A. Lim, Nat Methods **8**, 35 (2011).
[11]C. Hoffmann, E. Mazari, S. Lallet, R. Le Borgne, V. Marchi, C. Gosse, and Z. Gueroui, Nat. Nanotechnol. **8**, 199 (2013).
[12]C. Hoffmann, E. Mazari, C. Gosse, L. Bonnemay, S. Hostachy, J. Gautier, and Z. Gueroui, ACS Nano **7**, 9647 (2013).

[13]L. Bonnemay, S. Hostachy, C. Hoffmann, J. Gautier, and Z. Gueroui, Nano Lett. **13**, 5147 (2013).
[14]T. Wittmann, A. Hyman, and A. Desai, Nat. Cell Biol. **3**, E28 (2001).
[15]A. Desai, A. Murray, T. J. Mitchison, and C. E. Walczak, Methods Cell Biol. **61**, 385 (1999).
[16]J. Gaetz, Z. Gueroui, A. Libchaber, and T. M. Kapoor, Nat. Cell Biol. **8**, 924 (2006).
[17]M. Pinot, F. Chesnel, J. Z. Kubiak, I. Arnal, F. J. Nedelec, and Z. Gueroui, Curr. Biol. **19**, 954 (2009).
[18]P. Maddox, A. Straight, P. Coughlin, T. J. Mitchison, and E. D. Salmon, J. Cell Biol. **162**, 377 (2003).
[19]M. Shirasu-Hiza, Z. E. Perlman, T. Wittmann, E. Karsenti, and T. J. Mitchison, Curr. Biol. **14**, 1941 (2004).
[20]G. Yang, B. R. Houghtaling, J. Gaetz, J. Z. Liu, G. Danuser, and T. M. Kapoor, Nat. Cell Biol. **9**, 1233 (2007).
[21]E. Hannak and R. Heald, Nat. Protoc. **1**, 2305 (2006).
[22]H. C. Brinkman, Appl. Sci. Res. **1**, 27 (1949).
[23]C. T. Culbertson, S. C. Jacobson, and J. Michael Ramsey, Talanta **56**, 365 (2002).
[24]M. T. Valentine, Z. E. Perlman, T. J. Mitchison, and D. A. Weitz, Biophys. J. **88**, 680 (2005).
[25]E. D. Salmon, W. M. Saxton, R. J. Leslie, M. L. Karow, and J. R. McIntosh, J. Cell Biol. **99**, 2157 (1984).
[26]A. M. Jimenez, M. Roche, M. Pinot, P. Panizza, L. Courbin, and Z. Gueroui, Lab Chip **11**, 429 (2011).
[27]H. Salman, D. Zbaida, Y. Rabin, D. Chatenay, and M. Elbaum, Proc. Natl. Acad. Sci. U. S. A. **98**, 7247 (2001).
[28]T. U. Mayer, Science **286**, 971 (1999).
[29]See supplementary material at http://dx.doi.org/10.1063/1.4926324 for supplementary figures.
[30]M. Kirschner and T. Mitchison, Cell **45**, 329 (1986).
[31]E. Karsenti and I. Vernos, Science **294**, 543 (2001).
[32]M. Delattre and M.-A. Félix, Bioessays **31**, 537 (2009).